

Anomaly in the dielectric response at the charge orbital ordering transition of crystalline $\text{Pr}_{0.67}\text{Ca}_{0.33}\text{MnO}_3$

Silvana Mercone, Alexandre Wahl, Alain Pautrat, Michaël Pollet and Charles Simon

Laboratoire CRISMAT, CNRS UMR 6508, ENSICAEN-CNRS

6 Bd. du Maréchal Juin, 14050 Caen Cedex, France

(March 28, 2003)

The complex impedance has been measured in a $\text{Pr}_{0.67}\text{Ca}_{0.33}\text{MnO}_3$ polycrystalline sample. A strong frequency dependence is observed under zero magnetic field for a wide range of temperatures. This features is characteristic of relaxation process with a single Debye time relaxation constant. The anomaly observed in the dielectric constant and the peculiar type of ordering below T_{CO} , allows us to show that electric dipoles are present for $T < T_{\text{CO}}$.

I. INTRODUCTION

Mixed-valent manganites have been the focus of intense scientific activity over the past several years in view of the variety of physical phenomena they display as well as their potential for utilization in magnetic sensing and spin-polarized transport applications.¹

Of particular interest is the study of the behavior of the ordered state in these compounds. The competition between the charge-ordered (CO) insulating state, in which the electric charges are localized, and the charge-delocalized (CD) state, which presents a metallic-like conductivity, is of a great attention.^{2,3,4} The physics of this electronic phase transition are also linked to the magnetism of the system. The CO state is stabilized by an antiferromagnetic (AFM) ground state while that of the CD state is ferromagnetic (FM).⁵⁻⁷ Many experiments have shown that CO state is unstable under a variety of external perturbations including magnetic field,⁸⁻¹⁰ temperature, external and chemical pressure¹¹ (i.e. degree of cation/anion doping), x-ray¹² and electron¹³ irradiation. This CO state is also stabilized by the structural distortion of the perovskite lattice which often occurs upon A-cation doping. Among the various mixed-valence manganites studied so far, the $\text{Pr}_{1-x}\text{Ca}_x\text{MnO}_3$ (PCMO) system is particularly useful in studying the competition between the CO and CD states previously mentioned, as a result of the similar ionic radii of the A-site cations, which limit the distortion of the perovskite lattice upon doping.

In the last few years, experiments have focused on the effects of the application of an electric field on doped manganites. $\text{Pr}_{1-x}\text{Ca}_x\text{MnO}_3$ ($x=0.3, 0.33, 0.4$) bulk crystals,¹⁴ single crystals,^{15,16} ceramic samples¹⁷ and thin films,^{18,19} show similar results. All display a drop in the resistance above a threshold value of the applied DC-electric field (or DC-current). This electric-field-driven (or current-driven) insulator to metal transition gives rise to non-linear conductivity. The non-linearity of the I-V characteristics observed for $T < T_{\text{CO}}$ is explained by Guha *et al.*^{15,16} with a percolation process due to the melting of the CO-Insulating (COI) phase into the CD-Metallic one. This interpretation is based on the opening of metallic-filament paths in a COI-matrix. Stankiewicz *et al.*¹⁷ have rejected this explanation in manganites, as it is incompatible with the magnetic data they obtained under the application of a current. A filamentary picture of conductivity should result in no observable change in magnetization since, according to their calculations at the MI-transition, the FM volume is estimated to change only 0.05%. However, they observed a much larger variation. A more recent paper²⁰ has also shown the presence of the same non-linearity in a non-charge-ordered composition ($x=0.2$) in which the percolation model was not applicable.

To add to this scenario of differing views, recent spectroscopy experiments^{21,22} have suggested the development of a charge-density-wave (CDW). This is supported by the quasi-one-dimensional electronic structure proposed by Asaka *et al.*²³ in the light of their low-temperature TEM measurements. A. Wahl *et al.*²⁴ have also proposed the CDW theory in order to explain the I-V behavior of $\text{Pr}_{0.63}\text{Ca}_{0.37}\text{MnO}_3$. This phenomenological model was originally limited to the compound

NbSe₃,²⁵⁻³⁰ but was later generalized to a number of transition-metal compounds³¹ in order to explain the non-linear effects observed in their ac and dc transport properties. In order to complete the panorama of studies on this competition between the COI-AFM and CD-FM states, the preliminary study by Rivadulla *et al.*^{32,33} on the dielectric constant of Pr_{1-x}Ca_xMnO₃ should be mentioned. They found a large capacitive response of the material upon the appearance of the CO state. This effect is perhaps associated with the formation of electric dipoles below T_{CO}. They even suggest, in the light of their magnetization measurements, the existence of a strong FM-AFM competition for T<T_{N2}=160 K. As a consequence of AFM order in the CO state, hopping between the Mn sites is minimized so that the formation of the electric dipoles is permitted.

The aim of this report is to elucidate the nature of the electric-field induced conducting states of PCMO. We report complex impedance measurements of Pr_{0.67}Ca_{0.33}MnO₃ polycrystalline samples over four orders of magnitude of frequency and over a large range of temperatures (5 K- 400 K). The real part of the ac resistance (ReZ) shows a broad decrease at a crossover frequency which is highly dependent on temperature and at which the imaginary part of the impedance (ImZ) exhibits a peak. We have succeeded in reproducing this typical relaxation behavior using a Debye model for relaxation. The relaxation time is strongly dependent on temperature, and the dielectric constant displays an anomaly at T_{CO}.

II. EXPERIMENTAL

Using the floating-zone method with feeding rods of nominal composition Pr_{0.7}Ca_{0.3}MnO₃, a several cm-long single crystal was grown in an image furnace. The sample for measurement was cut from the middle part of this crystal. Electron dispersive spectroscopy analysis found the cationic composition to be x=0.33. Magnetization and dc-transport measurements were carried out in a SQUID magnetometer and in a PPMS-Quantum Design cryostat, respectively. Under zero magnetic field, the transport measurements show a classical insulating behavior with a resistivity up to 10⁹ Ωcm at 5 K. A change of slope can be observed at the onset of the charge ordering state. The characteristic temperatures are: T_{CO} about 225 K, T_C about 100 K and T_N about 115 K.³⁴

To measure the complex impedance of an insulating sample, it is necessary to eliminate any resonance phenomena between the resistance of the sample and the weak capacity of the cables for a given frequency. As the resistance is strongly temperature-dependent, it was necessary to use two different circuits depending on the temperature range in which the AC measurement are carried out. In both cases, the real and imaginary parts of the sample voltage were measured by a lock-in amplifier. The resistance of the sample was calculated using simple relations for the equivalent circuits.

The dielectric constant was measured directly at the highest temperatures (210 K-403 K) using a LCR Bridge (Flucke 6306). Due to the limits of the device, the lowest possible temperature for these measurements was 210 K. The sample was painted on both faces with In-Ga paste, and a 1 V AC-voltage was applied in the (50-1*10⁶) Hz range. Again, the contributions of the measured impedance, the air permittivity, the contacts and the cables (resistive and inductive effects) were carefully removed in order to obtain the actual permittivity of the sample.

III. RESULTS

In Figure 1, the modulus of $Z = \sqrt{ReZ^2 + ImZ^2}$ as a function of temperature is shown for frequencies ranging from 10 to 10⁵ Hz. As previously mentioned, the impedance of the sample varies strongly (several orders of magnitude) over the investigated range of temperatures; thus two circuits, depending on the temperature range, were used to carry out our measurements. The limit of validity of each circuit is denoted by the dashed line. The inset on the left side of Figure 1 shows the circuit for the low temperature (80K-120K); a constant voltage is applied and saturates when the resistance of the sample falls below R (R represents the saturation value of the circuit, R=100MΩ). The inset on the right side of Figure 1 shows the circuit used at high temperature (213K-403K). In this case a constant value of the current can be injected only if the resistance of the sample remains much lower than R. Solving in both cases the equivalent circuit, it is possible to observe the frequency dependence of the

complex impedance of the sample. This kind of behavior has already been observed by J. Sichelschmidt *et al.*³⁵, no interpretation was given to account for the data.

Figure 2(a) shows the modulus $Z = \sqrt{\text{Re}Z^2 + \text{Im}Z^2}$ of the complex impedance \bar{Z} at low temperature as a function of frequency. A significant frequency dependence of the impedance Z can be observed. A decrease of many orders of magnitude occurs when the frequency is increased. Both the crossover frequency ν_C (defined as the frequency where $Z = \frac{1}{\sqrt{2}} R_{DC}$) and the low-impedance value ($Z(\omega \rightarrow 0) = R_{DC}$) are clearly temperature-dependent.

Figure 2(b) displays the frequency dependence of Z investigated at high temperature. Several features are noteworthy. First of all, the impedance, which is rather low for these temperatures, is still frequency dependent and, more importantly the crossover frequency continues to be temperature dependent. In addition a critical change in the behavior of Z occurs between 253 K and 273 K. In this range of T there exists a crossover frequency above which Z begins to increase instead of decrease, as is observed at $T < 253$ K.

IV. ANALYSIS AND DISCUSSION

The above results are characteristic of a relaxational process. The real and imaginary parts of \bar{Z} present a crossover frequency at which the former starts to decrease and the latter exhibits a concurrent peak (Figures 3 and 4). This type of behavior has been quantitatively studied on CDW systems (such as NbSe₃ or the “blue bronze”) as a consequence of the excitation of a collective mode (CM).²⁵⁻³¹ The general feature of this complex model is to introduce an additional term to the normal conductivity of the system which deals with the CDW condensate. This term is frequency-dependent and can also be activated by a DC electric field with a threshold value (E_{Th} or I_{Th}). The equations generally used to explain the AC-transport in a CDW system are very general and can be used for any kind of system that presents a strong capacitive response.²⁴⁻³⁰

For the zero bias measurements, the amplitude of the voltage applied is much lower than the threshold value as defined in a DC measurement. The resistance, R_N , which in our AC-measurements drives the transport at low frequency, can be extrapolated from $Z(\omega)$ for $\omega \rightarrow 0$ (i.e. R_N). Thus the DC-resistance (R_N) of the sample is due to the “normal” electrons, i.e. the ones which are not condensed in the collective mode. According to R. J. Cava *et al.*,³¹ the frequency-dependent \bar{Z} , is then due to the condensate and it can be represented by a series of resistance-capacitance (R_{CM})-(C_{CM}) elements with a characteristic relaxation time (τ). In light of these considerations it is possible to model the observed ac-response with the equivalent electronic circuit shown in Figure 5(a). The overall sample \bar{Z} can be represented using a circuit where the resistance R_N is in parallel with an additional element that defines the capacitive response of the sample. In the limit $\mathbf{b} = \frac{R_{CM}}{R_N} \rightarrow 0$, we obtain the new linear-equivalent-circuit shown in Figure 5(b). The real and imaginary parts of the sample impedance are:

$$Z_{real}(\mathbf{w}) = \frac{R_N}{1 + \mathbf{t}_0^2 \mathbf{w}^2} \quad (1)$$

$$Z_{imaginary}(\mathbf{w}) = -[Z_{real}(\mathbf{w}) * \mathbf{t}_0 \mathbf{w}] \quad (2)$$

where $\mathbf{t}_0 = \mathbf{t}_p(\mathbf{b} \rightarrow 0) = \lim_{b \rightarrow 0} C \sqrt{R_N^2 + 2R_{CM}R_N - R_{CM}^2} = R_N C$

From the expressions above, one can note that the response obtained is that of a Debye relaxation process where the equivalent linear circuit is given by an RC one. The limit $\beta \rightarrow 0$ is verified whatever the temperature range, since $R_N = Z(\omega \rightarrow 0)$ is always larger than $R_{CM} = Z(\omega \rightarrow \infty)$ (Figure 2 (a) and (b)).

Using Equation (1), we fit the real part of $\bar{Z}(\omega)$ at various temperatures and then plug the obtained fit parameters (τ_0 and R_N) into Equation (2) to reproduce the imaginary part of $\bar{Z}(\omega)$. As seen in Figures 4 and 5 there is a good agreement between the model and the experimental data and this is observed within the whole temperature range. The solid squares in Figure 6 represent the relaxation time τ_0 calculated within the Debye model description.

In order to obtain more information about the temperature dependence of τ , let us return to Equation (1) and use the \bar{Z} measured at different frequencies as a function of the temperature. In the low frequency range (LF) where Z is constant, the response is only driven by the ‘normal’ electrons, i.e. $Z_{real}(\omega_{LF}) \rightarrow R_N$. Rearranging the Equation (1) and applying it for frequency $\omega_{HF} \gg \omega_{LF}$ results in:

$$\tau_0 = \frac{1}{\omega_{HF}} \sqrt{\frac{R_N}{Z_{real}(\omega_{HF})} - 1} \quad (3)$$

Through Equation (3) it is possible to reconstruct the low temperature dependence of the relaxation time (open circles in Figure 6). The high temperature dependence of the relaxation time curve cannot be obtained in this fashion since Equation (3) is only valid if $\frac{Z_{real}(\omega_{LF})}{Z_{real}(\omega_{HF})} \neq 1$. As seen in

Figure 6, the resulting values (opened circles) are in good agreement with the parameters of the fit for the Low Temperature (closed squares). From the log scale in Figure 6, it is apparent that the observed process does not exhibit a temperature-activated law through the whole range of T . In the high temperature regime (213 K-393 K), the Arrhenius law is obeyed with the activating energy $E_a \approx 31.14$ meV, which is of the same order of magnitude as that found by Rivadulla *et al.* in the same range of temperature.^{32,33} In the low temperature region (80 K-120 K), the relaxation time always follows an activated law but the slope has changed. In this case the activating energy found is $E_a \approx 20.37$ meV. The crossover temperature between the two regions is found to be $T \approx 135$ K. This dramatically illustrates the strong temperature dependence of the relaxation time constant which is not a trivial feature. Rivadulla *et al.*^{32,33} observed a frequency splitting in the dielectric constant of the same doped (PrCa) system below 160 K, the temperature at which their susceptibility measurements show a second antiferromagnetic transition. According to these authors, this complex relaxation behavior is probably due to some sort of magnetic frustration linked to an AFM-FM competition.

In order to shine light on the role of the magnetic and/or charge ordered state on the capacitive intrinsic response of PCMO, we have translated the complex impedance into a dielectric constant. An additional difficulty occurs since at high temperature, it is necessary to add to the capacitive model an inductive term to take into account the increase of the impedance above T_{CO} . The inductive contributions arising from contact pads are normally observed at higher frequency (>10 MHz), nevertheless, since the aim of the present study is the characterization of the capacitive effect, we will not develop this specific point in the following.

The analysis done up to now gives us the values of the capacitance of the PCMO as a function of the temperature. The permittivity is calculated through $\epsilon = \frac{Ce}{s\epsilon_0}$, e being the thickness of the

sample crossed by the current, ϵ_0 the vacuum dielectric constant and s the electrode surface. The inductive term introduced to explain the high temperature behavior ($T > T_{CO}$) of Z (see figure 2(b)), decreases as the temperature decreases. Its value is zero for all the curves below $T_{CO} \approx 230$ K. Thus, for $T < T_{CO}$ we recover the classical RC circuit according to the Debye relaxation process. The dielectric constant so obtained is shown as a function of the temperature in Figure 7. The first important feature of these curves is that there is a peak in the $\epsilon(T)$ at $T_{CO} = 225$ K. The second one is the absence of any large anomaly at the magnetic transitions in $\epsilon(T)$. It can be also noticed that the dielectric constant is not zero in the low temperature phase, whereas it is vanishing in the high temperature limit. All these features strongly suggest that we are in presence of a electric dipolar transition at T_{CO} with a diverging permittivity at the phase transition.

Let us now come back on the exact nature of the superstructure of such compounds. It was proposed from a detailed analysis of coupled X-Ray and neutron diffraction data that in the CE type

structure, the extra charge is not localized on the Mn ions (Figure 8 (a)) as it should be in a “charge ordered state” but on the orbitals (“orbital ordering”) as in a Zener polarons model⁶(Figure 8 (b)). D. Khomskii³⁷ has recently proposed that the charge could be rather localized between charge and orbital as shown in Figure 8 (c). This could lead to the presence of dielectric dipoles (for $T < T_{CO}$) which would give rise to an anomaly of the dielectric constant at T_{CO} . This is clearly what we observed in Figure 7. It should be reminded that the Khomskii model of dipoles was first proposed for the CE type structure of half doped system and that the model of Zener polarons based on this latter was successfully applied to the PCMO(x=0.4). Here, we see that it seems also efficient to explain the behavior of the permittivity of the PCMO(x=0.33).

Another important feature in Figure 7 is the absence of any anomaly at the magnetic transition temperature. This can be explained by considering a system which would not be sufficiently frustrated. The only effect driven by the magnetic phase which can be detected by these measurements is the crossover in the temperature dependence of the relaxation time seen in the $\tau\left(\frac{1}{T}\right)$ curves below $T=135$ K, as it was established before. The study of the magnetic phase separation and its influence on the observed relaxation phenomena has been studied in more detail and will be published elsewhere. In addition, it should be also pointed out that the features observed in DC measurements (non linear behavior), can also be explained by the depinning of the dipole ordering³⁸ which is similar to what is observed in CDW depinning.²⁴

V. CONCLUSION

In conclusion the complex impedance has been measured in a $\text{Pr}_{0.67}\text{Ca}_{0.33}\text{MnO}_3$ polycrystal. A strong frequency dependence is observed under zero magnetic field for a wide range of temperatures. This feature is characteristic of a relaxation process with a single Debye time relaxation constant. The Z of a linear-equivalent-circuit is in good agreement with the experimental data. This type of behavior can be interpreted, on one hand, in the frame of CDW condensate depinning as the equations generally used to explain the transport in a CDW system are very general and can be used for any kind of system which present a strong capacitive response. On the other hand this kind of behavior is exactly the same observed in the polarized systems where the condensate is due to electric dipoles. The anomaly observed in the dielectric constant and the peculiar type of ordering below T_{CO} , is in agreement with the suggested existence of a dipolar structure in this temperature domain. The magnetic transition of the sample for $T < 135$ K causes a change of the slope in the time constant temperature dependence.

VI. ACKNOWLEDGMENTS

We acknowledge L. Hervé and M. Strelbel Morin for sample preparation and D. Khomskii, M.B. Weissman and V. Caignaert for useful discussions we had the opportunity to have with them. S. Mercone is supported by a Marie Curie fellowship of the European Community program under contract number HPMT2000-141.

REFERENCES

- ¹For a review, see for example “*Colossal Magnetoresistive Oxides*”, edited by Y.Tokura (Gordon and Breach Science, New York, 1998), “*Metal-insulator transitions*”, M.Imada, A.Fujimori and Y.Tokura (Reviews of Modern Physics Oct. 1998), “*The Physics of manganites: Structure and transport*”, M.B.Salamon and M.Jaime (Reviews of Modern Physics, July 1998) and “*Colossal Magnetoresistant materials: the key role of phase separation*”, E.Dagotto, T.Hotta and A. Moreo (Physics-Reports, April 2001).
- ²P.Shiffer, A.P. Ramirez, W. Bao, S.-W. Cheong, Phys. Rev. Lett. **75**, 3336 (1995).
- ³A. Urushibara, Y. Moritomo, T. Arima, A. Asamitsu, G. Kido, Y. Tokura, Phys. Rev. B **51**, 14103 (1995).
- ⁴G. Varelogiannis, Phys. Rev. Lett. **85**, 4172 (2000).
- ⁵T. Hotta and E. Dagotto, Phys. Rev. B **61**, R11879 (2000).

- ⁶ I.V. Soloveyev, Phys. Rev. B **63**, 174406 (2001).
- ⁷ S.Shimomura, T. Tonegawa, K. Tajima, N. Wakabayashi, N. Ikeda, T. Shobu, Y. Noda, Y. Tomioka and Y. Tokura, Phys. Rev. B **62**, 3875 (2000).
- ⁸ H. Yoshizawa, H. Kawano, Y. Tomioka, Y. Tokura, Phys. Rev. B **52**, R13145 (1995).
- ⁹ A.Anane, J.-P. Renard, L. Reversat, C. Dupas, and P. Veillet, M. Viret, L. Pinsard and A. Revcolevschi, Phys. Rev. B **59**, 77 (1999).
- ¹⁰ Y. Tomioka *et al.*, Phys. Rev. B **53**, R1689 (1996).
- ¹¹ Y. Moritomo, H. Kuwahara, Y. Tomioka and Y. Tokura, Phys. Rev. B **55**, 7549 (1997).
- ¹² V. Kiryukhin *et al.*, Nature (London) **386**, 813 (1997).
- ¹³ M. Hervieu, A. Barnabé, C. Martin, A. Magnan and B. Raveau, Phys. Rev. B **60**, R726 (1999).
- ¹⁴ A. Asamitsu, Y. Tomioka, H. Kuwahara and Y. Tokura, Nature (London) **388**, 50 (1997).
- ¹⁵ A.Guha, A.Raychaudhuri, A.R. Raju and C.N.R.Rao, Phys.Rev.B **62**, 5320 (2000).
- ¹⁶ A.Guha, N.Khare, A.Raychaudhuri and C.N.R.Rao, Phys.Rev.B **62**, R11941 (2000).
- ¹⁷ J. Stankiewicz, J. Sesé, J. Garcia, j. Blasco and C. Rillo, Phys.Rev.B **61**, 11236 (2000).
- ¹⁸ S. Srivastava, N. K. Pandey, P. Pandey, P. Padhan and R.C. Budhani, Phys.Rev.B **62**, 13868 (2000).
- ¹⁹ C.N.R. Rao, A.R. Raju, V.Ponnambalam, S.Parashar and N.Kumar, Phys.Rev.B **61**, 594 (2000).
- ²⁰ S. Mercone, A. Wahl, Ch. Simon and C. Martin, Phys.Rev.B **65**, 214428 (2002).
- ²¹ N. Kida and M. Tonouchi, Phys.Rev.B **66**, 024401 (2002).
- ²² P. Calvani, G. De Marzi, P. Dore, S. Lupi, P. Maselli, F. D'Amore, S. Gagliardi and S-W. Cheong, Phys. Rev. Lett **81**, 4504 (1998).
- ²³ T. Asaka, S. Yamada, S. Tsutsumi, C. Tsuruta, K. Kimoto, T. Arima and Y. Matsui, Phys. Rev. Lett. **88**, 097201 (2002).
- ²⁴ A. Wahl, S. Mercone, A. Pautrat, M. Pollet, Ch. Simon and D. Sedmidubsky, submitted to Phys. Rev. B.
- ²⁵ P.Monceau, J. Richard and M. Renard, Phys. Rev. B. **25**, 931 (1982).
- ²⁶ J. Richard, P.Monceau and M. Renard, Phys. Rev. B. **25**, 948 (1982).
- ²⁷ G. Grüner, A. Zawadowski and P.M. Chaikin, Phys. Rev. Lett. **46**, 511 (1981).
- ²⁸ R.M. Fleming and C.C. Grimes, Phys. Rev. Lett. **42**, 1423 (1979).
- ²⁹ P.Monceau, N.P. Ong, A.M. Portis, A. Meerschaut and J. Rouxel, Phys. Rev. Lett. **37**, 602 (1976).
- ³⁰ N.P. Ong and P.Monceau, Phys. Rev. Lett. **16**, 3443 (1977).
- ³¹ R.J. Cava, R.m. Fleming, P. Littlewood, E.A. Rietman, L.F. Schneemeyer and R.G. Dunn, Phys. Rev. B **30**, 3228 (1984).
- ³² F.Rivadulla, M.A. Lopez-Quintela, L.E. Hueso, C. Jardon, A. Fondado, J. Rivas, M.T. Causa and R.D. Sanchez, Solid State Communications 110 (1999) 179-183.
- ³³ C. Jardon, F.Rivadulla, L.E. Hueso, A. Fondado, M.A. Lopez-Quintela, J. Rivas, R. Zysler, M.T. Causa and R.D. Sanchez, J. Mag.Mag.Mat. 196-197 (1999) 475-476.
- ³⁴ Ch. Simon, S.Mercone, N. Guiblin, C. Martin, A. Brulet and G. André, Phys. Rev. Lett. **89**, 207202 (2002)
- ³⁵ J. Sichelschmidt, M. Paraskevopoulos, M. Brando, R. Wehn, D. Ivannikov, F. Mayr, K. Pucher, J. Hemberger, A. Pimenov, H.-A. Krug von Nidda, P. Lunkenheimer, V. Yu. Ivanov, A. A. Mukhin, A. M. Balbashov and A. Loidl, Eur. Phys. J. B **20**, 7-17 (2001).
- ³⁶ A. Daoud-Aladine, J. Rodriguez-Carvajal, L. Pinsard-Gaudart, M. T. Fernández-Diaz, and A. Revcolevschi, Phys. Rev. Lett. **89**, 097205 (2002).
- ³⁷ D. Khomskii, private communication.
- ³⁸ T. Tybell, P. Paruch, T. Giamarchi, J.M. Triscone, Phys. Rev. Lett. **89**, 097601 (2002).

FIGURES

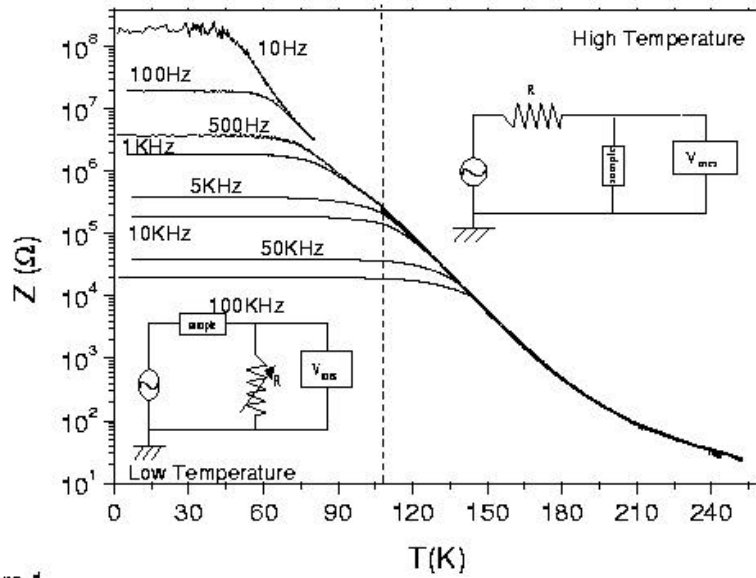


Figure 1
S.Mercone et al.

Figure 1: The modulus $Z = \sqrt{ReZ^2 + ImZ^2}$ of the complex impedance of the sample in function of temperature at different frequencies. Left inset: the circuit used at low temperature, which works at constant voltage and which saturates when the resistance of the sample and R are of the same order of magnitude. Right inset: the circuit used at high temperature, which works at constant current only if the resistance of the sample is lower than R.

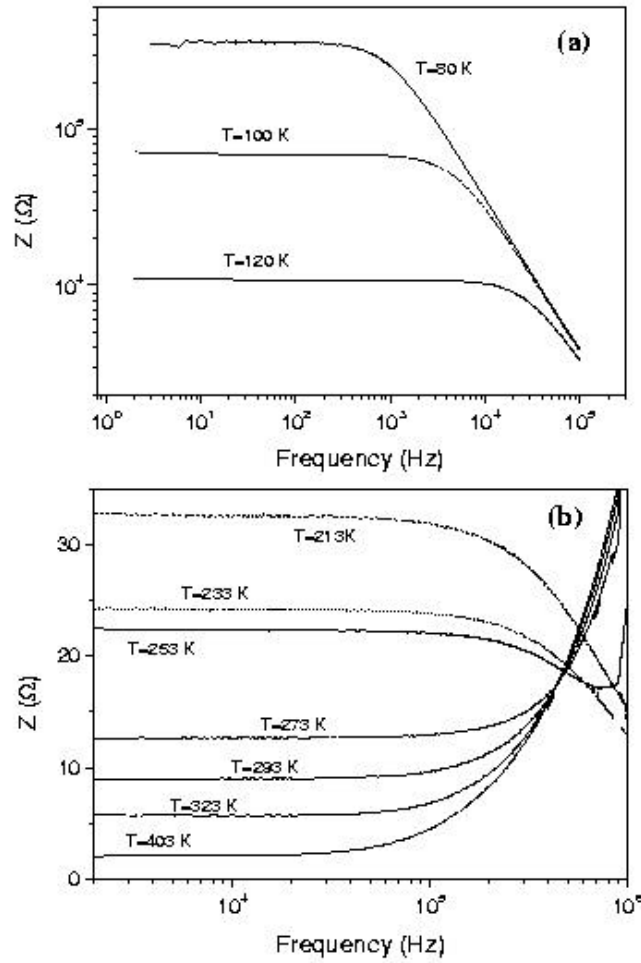


Figure 2
S.Mercone et al.

Figure 2: The modulus Z of the complex impedance as a function of the frequency at (a) low T (b) and high T . The threshold frequency and the impedance in the DC limit ($Z(\omega \rightarrow 0)$) clearly change as a function of temperature. The behavior of Z changes drastically between 253 K and 273 K.

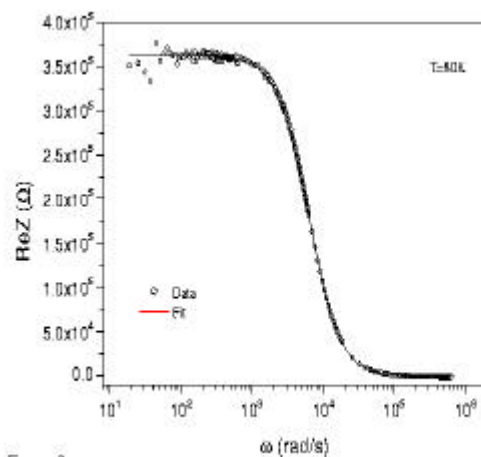


Figure 3
S. Mercone et al.

Figure 3: Real part of the complex impedance \bar{Z} as a function of the pulse ω at $T=80$ K. Open circles are the experimental data and line corresponds to the fit from Equation (1). The values of the parameters found are: $\tau_0=(1.6 \cdot 10^{-4}) \text{ sec}^{-1}$ and $R_N \approx (3.6 \cdot 10^5) \Omega$.

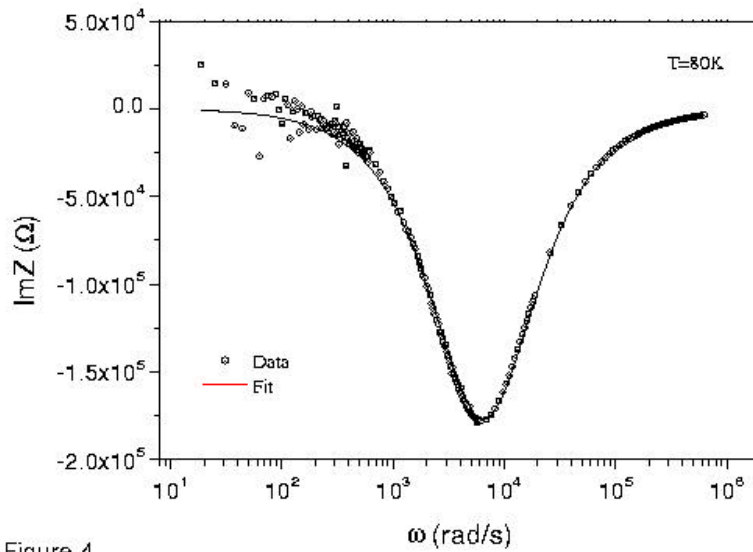


Figure 4
S.Mercone et al.

Figure 4: Imaginary part of the complex impedance \bar{Z} as a function of the pulse ω at $T=80$ K. Open circles are the experimental data and the line corresponds to the simulation by Equation (2) using the parameters from the fit of the $Z_{\text{real}}(\omega)$ (figure 3).

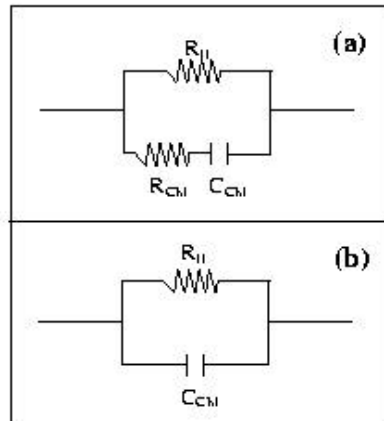


Figure 5
S.Mercone et al.

Figure 5 (a) Equivalent circuits used to simulate the electrical response of the sample : R_N = resistance of the normal electrons, R_{CM} and C_{CM} =, resistance and capacity, respectively of the electrons condensed in the collective mode. (b) The previously equivalent circuit within the limit

$$b = \frac{R_{CM}}{R_N} \rightarrow 0.$$

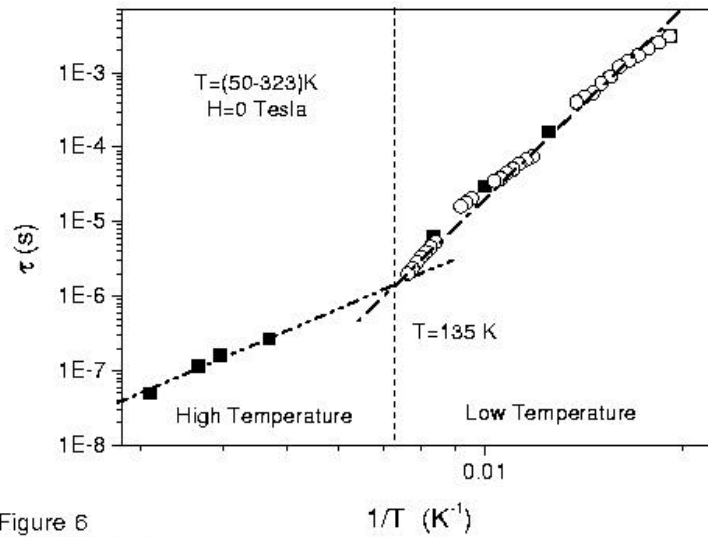


Figure 6
S.Mercone et al.

Figure 6: Relaxation time, τ , as a function of the reciprocal temperature. Closed squares are obtained from the fit (Equation (1)) and opened circles from the Equation (3).

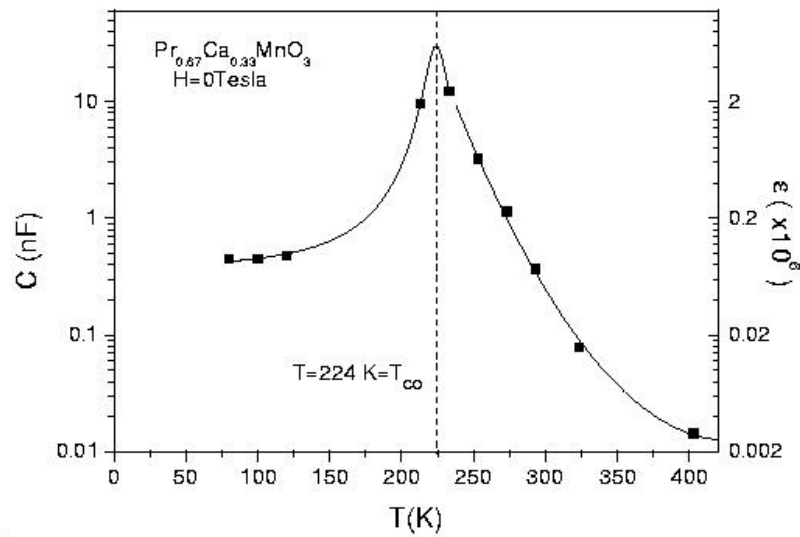


Figure 7
S.Mercone et al.

Figure 7: Permittivity of PCMO as a function of temperature.

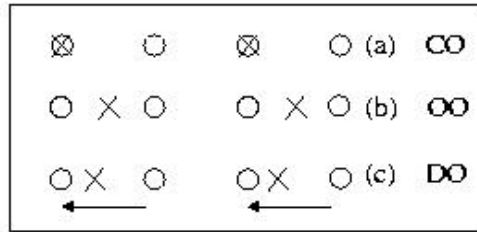


Figure 8
S. Mercone et al.

Figure 8 : Schematic drawing of: (a) Charge Ordering; (b) Orbital Ordering; (c) Dipole Ordering. The circles point the atomic positions and the crosses the charge ones.